# Robust Track-Following Controller Design in Hard Disk Drives Based on Parameter Dependent Lyapunov Functions

Richard Conway[1], Jongeun Choi[2], Ryozo Nagamune[3], and Roberto Horowitz[1]

[1]Department of Mechanical Engineering, University of California, Berkeley, CA 94720-1740 USA
[2]Departments of Mechanical Engineering, and Electrical and Computer Engineering, Michigan State University, East Lansing, MI 48824-1226 USA
[3]Department of Mechanical Engineering, University of British Columbia, Vancouver, BC V6T 1Z4, Canada

This paper presents a novel technique for designing robust track-following output-feedback controllers in hard disk drives (HDDs). In this paper, the manufacturing variations of HDDs are modeled as polytopic parametric uncertainties in linear time-invariant discrete-time systems. For this model, the robust track-following control problem is formulated as the worst-case $\mathcal{H}_2$ performance optimization. The optimization problem reduces to the one with bilinear matrix inequalities (BMIs), using the parameter dependent Lyapunov functions and the extended LMI condition introduced by de Oliveira. Although the formulated problem is nonconvex, and thus it is difficult to ensure global optimality, a numerical technique called "$\mathcal{G}$-$K$ iteration" is applied for optimization to guarantee monotonic non-increase of the worst-case performance during iterations. The proposed design technique will be useful in improving the track-following performance, and thus increasing the storage capacity of HDDs.

*Index Terms*—Hard disk drives, LMI optimization, robust track-following controller.

## I. INTRODUCTION

TO increase the capacity of hard disk drives (HDDs), the track density has to be increased. Researchers in the HDD industry estimate the track density for the future storage density to be about 1 000 000 track-per-inch (TPI), requiring a track mis-registration (TMR) budget of less than 2.5 nm $(3\sigma)$. To achieve this future goal, higher control bandwidth is necessary to gain sufficient positioning accuracy of the read/write head position with respect to the track which will be referred to as the position error signal (PES) [1], [2]. To overcome this challenge, a class of dual-stage actuators for HDDs has been proposed [3]–[8]. A microactuator (MA) is placed at the end of the suspension and moves the slider/head relative to the suspension tip, increasing servo bandwidth [9]. A dual-stage servo system using enhanced active-passive piezoelectric actuators was proposed in [7]. Reliability evaluation of piezoelectric MAs in HDDs were reported in [8]. A dedicated sensor system using piezoelectric strain gages for detecting vibration on the sensor arm directly has been developed in [10], which enables high-frequency sampling and modal selectivity. Sensing techniques for *in situ* measurement of head-slider in both flying height and off-track directions have been developed in [11].

The control objective in robust track-following is to obtain a small RMS value of the PES against all undesirable exogenous disturbance such as track runout, windage, and measurement noise over all HDD products with dynamics variations [12]. A method to achieve this objective is to mathematically model such disturbance and dynamics variations, and then to design a robust $\mathcal{H}_2$ controller [13]. A parameter uncertainty identification technique for robust $\mathcal{H}_2$ control synthesis was reported in [14]. A tradeoff between performance and controller complexity in HDDs was addressed by control-oriented modeling

and robust control [15]. An alternative approach that classifies the disk drives into several sets depending on dynamics properties, and applies a single robust controller to each set has been proposed by [16]. Another way to deal with model uncertainty is to use adaptive control schemes. An adaptive disturbance rejection scheme in HDDs has been introduced in [17]. A neural-networks-based adaptive disturbance rejection technique for HDDs has been developed in [18]. Online iterative control has been used to cope with nonrepeatable run-out disturbances in HDDs [19].

In this paper, we consider a single robust $\mathcal{H}_2$ controller to deal with parametric uncertainties in HDDs [13], [20]. The problem of designing an optimal full-order output-feedback controller for polytopic uncertain systems can be formulated as an optimization problem subject to a set of bilinear matrix inequalities (BMIs). However, in general, the optimization subject to a set of BMIs, which is non-convex, is difficult to solve. In the case of a relatively high order uncertain system, most of the global approaches to the solution of the BMI problem are not practical due to the resulting large number of variables that enter bilinearly in matrix inequalities [21]. On the other hand, several local search optimization algorithms have been proposed [22], [23] that are computationally fast enough to deal with this problem. A straightforward local approach takes advantage of the fact that, by fixing a set of the bilinearly-coupled variables, the BMI problem becomes a convex optimization problem in the remaining variables and vice versa. The algorithm iterates among two LMI optimization problems. In each LMI problem a set of bilinearly-coupled variables is kept constant and the minimum is searched among their bilinear conjugates. The iterative algorithm is stopped when this search reaches a local minimum or a reasonably low performance cost is achieved. A coordinate descent method that utilizes the dual iterative approach for BMI problems was proposed in [23]. Unfortunately, the convergence properties of this type of dual iteration approach is sensitive to the initial condition and the tolerances of the numerical LMI solvers. Moreover, in general, these algorithms are not guaranteed to converge to the globally optimal solution nor to a locally optimal solution for the originally formulated BMI problem.

However, the dual iterative approach has been successfully utilized to synthesize robust controllers for track-following hard disk drive servo systems with dual-stage actuators [12] and multirate and multi-sensing track-following servo systems in HDDs [24], [25], [20]. Therefore, in many applications these types of algorithms appear to be effective in the design of fixed order robust controllers for parametrically uncertain systems with relatively high orders.

This paper presents a so-called "$\mathcal{G}$-$K$" iteration technique for robust track-following controller design in HDDs. In particular, this dual iterative descent algorithm is based on parameter dependent Lyapunov functions. The proposed algorithm achieves better worst-case performance than the one used in [12], [24], and [25] but requires more computational power in solving controller design problems. Specifically, a robust output-feedback controller is optimized for the worst-case performance of a linear time invariant (LTI) discrete-time system under convex polytopic parametric uncertainties, based on the extended LMI condition with an instrumental variable "$\mathcal{G}$" introduced by de Oliveira [26]. Using this condition, a new dual iterative algorithm is presented, which is henceforth called the "$\mathcal{G}$-$K$ iteration" algorithm as compared to the "$P$-$K$ iteration" used in [12], [24], and [25]. It will be shown that this algorithm updates the controller parameters in order to guarantee monotonic non-increasing worst-case performance.

This paper is organized as follows. At the end of this section, we first introduce notation which appears in the paper. In Section II, we introduce a nominal plant for a HDD servo with a translational MEMS actuator and parameter variations. We also present the generalized plant that consists of the nominal plant and uncertain parameters for which a single robust discrete-time robust controller needs to be designed. In Section III-A, polytopic parametric uncertain LTI systems are introduced in a general context. Section III-B formulates the worst-case $\mathcal{H}_2$ performance minimization problem for a polytopic parametric uncertain LTI system. For the formulated problem, descent algorithms called "$P$-$K$ iteration" and "$\mathcal{G}$-$K$ iteration" are presented in Section III.C to design robust controllers based on LMI techniques. An illustrative example is presented in Section IV, where the algorithms discussed in Section III are used to design a robust $\mathcal{H}_2$ track-following controller for the dual-stage servo system with variations introduced in Section II.

The notation in this paper is standard. $\mathbb{R}^{n \times m}$ is the set of real $n \times m$ matrices. $\mathbb{R}^n$ is the set of real $n$ dimensional vectors. $I_{n \times n}$ denotes the identity matrix of size $n$ and $0_{n \times m} \in \mathbb{R}^{n \times m}$ represents an $n \times m$ zero matrix. The direct sum of two matrices $A \in \mathbb{R}^{m \times m}$ and $B \in \mathbb{R}^{n \times n}$ is denoted as $A \oplus B :=$ $\mathrm{diag}(A, B) \in \mathbb{R}^{(m+n) \times (m+n)}$, which is a block diagonal matrix, and having main diagonal blocks square matrices $A$ and $B$, such that the off-diagonal blocks are zero matrices. A transfer function of a discrete-time LTI system is denoted by

$$\left[ \begin{array}{c|c} A & B \\ \hline C & D \end{array} \right] := D + C(zI - A)^{-1}B. \qquad (1)$$

Other notation will be explained in due course.

## II. ROBUST TRACK-FOLLOWING CONTROL PROBLEM IN HDDS

In this section, we first present a nominal plant for a HDD servo with a translational MEMS actuator and the associated
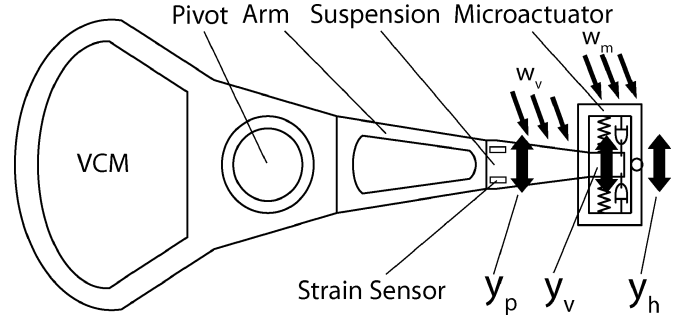

Fig. 1. Schematic of a dual stage HDD servo system with a translational MEMS actuated slider.
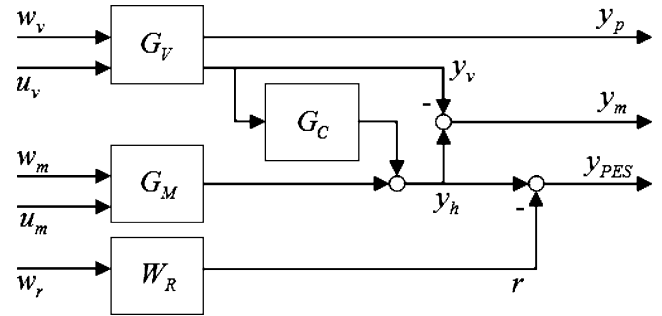

Fig. 2. Block diagram of a dual stage HDD servo system with a translational MEMS actuated slider.

generalized plant that consists of the nominal plant and uncertain parameters. The plant model has been used in the literature [20], and considered to be realistic enough.

We consider a specific example here, but the controller design technique to be proposed in Section III is general enough to cover track-following servo control problems for various configurations in HDDs (such as single-stage, suspension-actuated or slider-actuated dual-stage, and multi-sensing).

### A. Dual-Stage Servo Systems With a Translational MEMS Actuator

We consider a dual-stage HDD servo system with a translational MEMS actuated slider, the schematic and block diagram of which are respectively shown in Figs. 1 and 2.

The control inputs are electrical signals to the voice coil motor (VCM) and the microactuator (MA), denoted by $u_v$ and $u_m$ respectively. The airflow disturbance signals to VCM and MA, $w_v$ and $w_m$ respectively, are assumed to be modeled as the normalized Gaussian white noise. The signals $y_h, y_p, y_v$, and $y_m$ are respectively the read/write head position, the output of a strain sensor mounted on the suspension, the suspension tip displacement, and the position of the MA relative to the suspension tip displacement. The track runout signal, $r$, models the desired head motion relative to the tracks on the disk resulting from mechanical imperfections, D/A quantization noise, and power-amp noise. $y_{PES}$ is the position error signal (PES), which is defined as the position of the read/write head with respect to the track. The controller has access to measurements of $y_p, y_m$, and $y_{PES}$, each of which is contaminated by its respective Gaussian white measurement noise signal. The transfer functions for the VCM dynamics $G_V$, the MA dynamics $G_M$, and the coupling between

TABLE I
NOMINAL PARAMETER VALUES

| q | mode | Parameter | | |
|---|------|-----------|---|---|
|   |      | $\zeta_q$ | $\bar{\omega}_q$ | $A_q$ |
| 1 | rigid body and friction | 0.5 | 376.99 | $\left( \begin{bmatrix} 0 \\ 4.461 \end{bmatrix} \begin{bmatrix} 0 & 4.461 \end{bmatrix} \right) \times 10^8$ |
| 2 | butterfly | 0.015 | $4.6533 \times 10^4$ | $\left( \begin{bmatrix} 2.644 \\ -4.626 \end{bmatrix} \begin{bmatrix} 3.595 & 3.932 \end{bmatrix} \right) \times 10^8$ |
| 3 | sway | 0.015 | $6.7272 \times 10^4$ | $\left( \begin{bmatrix} 7.636 \\ -6.209 \end{bmatrix} \begin{bmatrix} -9.596 & 2.185 \end{bmatrix} \right) \times 10^8$ |
| 4 | torsional | 0.015 | $3.3171 \times 10^4$ | $\left( \begin{bmatrix} 2.612 \\ 0.95 \end{bmatrix} \begin{bmatrix} 0 & -2.78 \end{bmatrix} \right) \times 10^6$ |
| 5 | torsional | 0.015 | $5.7499 \times 10^4$ | $\left( \begin{bmatrix} 3.171 \\ -5.391 \end{bmatrix} \begin{bmatrix} 0 & 6.255 \end{bmatrix} \right) \times 10^6$ |
| 6 | torsional | 0.015 | $8.1759 \times 10^4$ | $\left( \begin{bmatrix} 1.959 \\ -3.359 \end{bmatrix} \begin{bmatrix} -3.822 & 0.717 \end{bmatrix} \right) \times 10^8$ |
| 7 | torsional | 0.015 | $9.5562 \times 10^4$ | $\left( \begin{bmatrix} -2.271 \\ 2.571 \end{bmatrix} \begin{bmatrix} 3.411 & 0.362 \end{bmatrix} \right) \times 10^8$ |
| m | miro-actuator | 0.2 | $1.4162 \times 10^4$ | $\begin{bmatrix} 1.199 & 0.04 \end{bmatrix} \times 10^9$ |

the VCM and MA dynamics $G_C$, are respectively represented as

$$G_V(s) := \sum_{i=1}^{7} \frac{A_i}{s^2 + 2\zeta_i \omega_i s + \omega_i^2},$$

$$G_M(s) := \frac{A_m}{s^2 + 2\zeta_m \omega_m s + \omega_m^2},$$

$$G_C(s) := \frac{2\zeta_m \omega_m s + \omega_m^2}{s^2 + 2\zeta_m \omega_m s + \omega_m^2} \qquad (2)$$

where $A_i$ and $A_m$ are static gain matrices for $G_V(s)$ and $G_m(s)$ respectively given by

$$A_i := \begin{bmatrix} a_{w_v \to y_p} & a_{u_v \to y_p} \\ a_{w_v \to y_v} & a_{u_v \to y_v} \end{bmatrix} \quad \text{for } i \in \{1, \ldots, 7\},$$

$$A_m := \begin{bmatrix} a_{w_m \to y_m} & a_{u_m \to y_m} \end{bmatrix}.$$

The low-frequency nature of track runout is characterized by

$$r(s) := \underbrace{\left[ \frac{2.8 \times 10^9}{s^2 + 800s + 2.5 \times 10^5} + \frac{1.2 \times 10^5}{s + 1.9 \times 10^3} \right]}_{=:W_R(s)} w_r(s)$$

where $w_r(s)$ is normalized Gaussian white noise.

### B. Parametric Uncertainties in Dual-Stage Servo Systems

For the model introduced in (2), we assume that although the values of $\zeta_1, \omega_1$, and $A_i$ are known, the remaining parameters can vary up to the amounts shown in Table II. With these assumptions, we express the parametric uncertainties in the relevant continuous-time transfer function coefficients as

$$\begin{aligned}
\zeta_1 \omega_1 &= \bar{\zeta}_1 \bar{\omega}_1, & \omega_1^2 &= \bar{\omega}_1^2, \\
\zeta_i \omega_i &= \bar{\zeta}_i \bar{\omega}_i (1 + 0.14\lambda_{c1i}), & \omega_i^2 &= \bar{\omega}_i^2 (1 + 0.08\lambda_{c2i}), \\
i &= 2, \ldots, 7 \\
\zeta_m \omega_m &= \bar{\zeta}_m \bar{\omega}_m (1 + 0.16\lambda_{c1m}), & \omega_m^2 &= \bar{\omega}_m^2 (1 + 0.12\lambda_{c2m})
\end{aligned}$$

TABLE II
PARAMETER VARIATIONS IN THE FULL MODEL

|       | $\zeta$ | $\omega$ |
|-------|---------|----------|
| $G_V$ | $\pm 10\%$ | $\pm 4\%$ |
| $G_M$ | $\pm 10\%$ | $\pm 6\%$ |

where parameters with "overbar" are nominal ones listed in Table I, and the values of the $\lambda$s are unknown, but known to lie in the interval $[-1, 1]$. It should be noted that we introduced some conservatism into the model for the $\zeta$s in order for the transfer function coefficients to depend affinely on the unknown parameters. The resulting model, which we will denote $\bar{\Sigma}_C^{\bar{\Lambda}_c}$, is 19th-order with 14 parametric uncertainties.

To reduce the amount of computation time required to synthesize a controller and the complexity of the resulting controller, it is necessary to simplify the model as much as possible before performing the controller design. Thus, we only consider the first three terms in $G_V$ during control design and make the restrictions that $\lambda_{c12} = \lambda_{c13} = \lambda_{c22} = \lambda_{c23} =: \lambda_c$ and all other uncertainties are zero. These restrictions on the parametric uncertainties correspond to the assumption that the ratios between the quantities $\zeta_2, \zeta_3, \omega_2$, and $\omega_3$ are known. This technique was introduced in [27] to reduce the number of uncertain parameters by exploiting the correlation between physical parameters. With these simplifying assumptions, the system model is 11th order and contains one parametric uncertainty, $\lambda_c$. Defining $\Lambda_c := [-1, 1]$, Fig. 3 shows the open-loop Bode plot from $u$ to $y$ of this reduced model for 50 randomly selected values of $\lambda_c \in \Lambda_c$. The resulting order of the reduced-order system will be the order of the synthesized controller.

### C. Generalized Plant

The generalized plant that consists of the nominal plant and parametric uncertainties for the controller design is shown in Fig. 4. The inputs and outputs of the generalized plant are
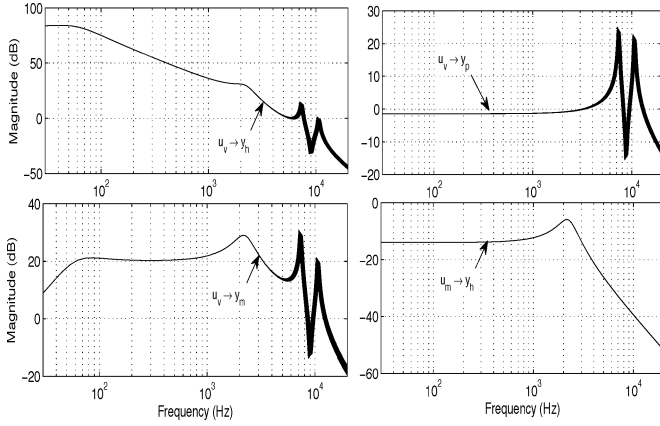
Fig. 3. The Bode plot of the reduced-order, continuous-time system from $u$ to $y$ for 50 random samples of $\lambda_c \in \Lambda_c$.



Fig. 5. The Bode plot of the reduced-order, discrete-time system from $u$ to $y$ for 50 random samples of $\lambda \in \Lambda$.
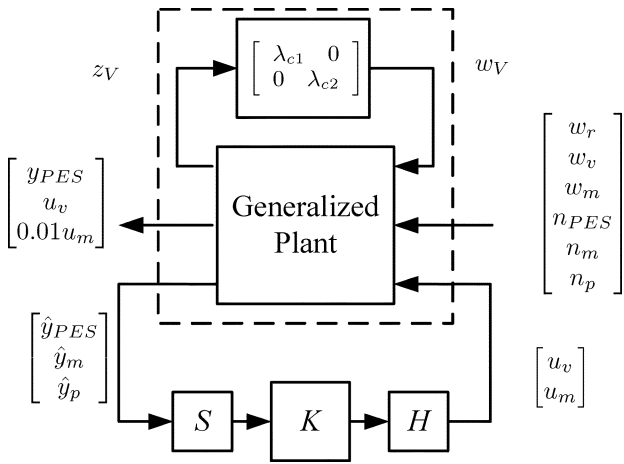


Fig. 4. The generalized plant with parametric uncertainties for the controller design. $S$ is the sampler and $H$ is the zero-order hold.

chosen as

$$z := \begin{bmatrix} y_{\text{PES}} \\ u_v \\ 0.01 u_m \end{bmatrix}, \quad w := \begin{bmatrix} w_r \\ w_v \\ w_m \\ n_{\text{PES}} \\ n_m \\ n_p \end{bmatrix},$$

$$y := \begin{bmatrix} \hat{y}_{\text{PES}} \\ \hat{y}_m \\ \hat{y}_p \end{bmatrix}, \quad u := \begin{bmatrix} u_v \\ u_m \end{bmatrix}$$

where $\hat{y}_{\text{PES}}, \hat{y}_m$, and $\hat{y}_p$ are output measurements, respectively corrupted by Gaussian white noise signals $n_{\text{PES}}, n_m$, and $n_p$, i.e.,

$$\hat{y}_{\text{PES}} = y_{\text{PES}} + n_{\text{PES}},$$
$$\hat{y}_m = y_m + n_m,$$
$$\hat{y}_p = y_p + n_p.$$

In the controlled output signal $z$, the "weight" 0.01 on $u_m$ was selected by trial and error.

### D. Robust Track-Following Control Problem

The objective of our work is to design a single $\mathcal{H}_2$ robust controller to attenuate the variances of the PES and control ef-
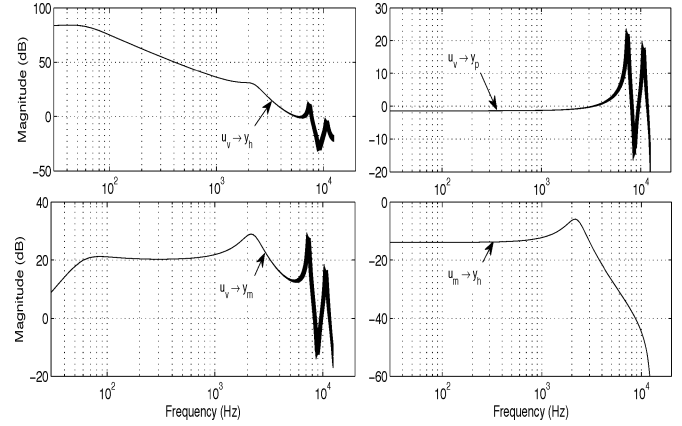
forts against the disturbance for the plant with the parameter variations. The generalized plant along with the controller for this purpose is formulated and shown as in Fig. 4. In order to design the discrete-time controller, we discretize the continuous-time parameter uncertain system as follows. We first obtain corresponding system vertices in the uncertain parameter space, and discretize those vertices to form the discrete-time uncertain system, $\Sigma^\Lambda$. Fig. 5 shows the open-loop Bode plot from $u$ to $y$ of the reduced model for 50 randomly selected values of $\lambda \in \Lambda$. In this paper, we will design a single discrete-time robust controller for the convex combination of the discrete-time system vertices. The resulting discrete-time uncertain system will be elaborated further in the following section.

### III. WORST-CASE $\mathcal{H}_2$ PERFORMANCE MINIMIZATION VIA $\mathcal{G} - K$ ITERATION

In this section, first, polytopic parametric uncertain LTI systems are introduced in a general context. We then formulate the worst-case $\mathcal{H}_2$ performance minimization problem for a polytopic parametric uncertain LTI system. For the formulated problem, descent algorithms are presented to design robust controllers based on LMI techniques.

### A. Polytopic Parametric Uncertain LTI Systems

Let us consider a set $\Sigma^\Lambda$ of the discrete-time LTI generalized plant $[\Sigma^\lambda](z)$, shown in Fig. 6:

$$\Sigma^\Lambda := \left\{ [\Sigma^\lambda](z) := \left[ \begin{array}{c|cc} A(\lambda) & B_1(\lambda) & B_2(\lambda) \\ \hline C_1(\lambda) & D_{11}(\lambda) & D_{12}(\lambda) \\ C_2 & D_{21} & 0 \end{array} \right], \right.$$
$$\left. \lambda \in \Lambda \right\} \quad (3)$$

where the vector $\lambda \in \mathbb{R}^N$ represents an uncertain time-invariant parameter vector in an uncertainty set. In Fig. 6, $z$ (of dimension $n_z$) is the output of the system, $w$ (of dimension $n_w$) is the disturbance to the system, $u$ (of dimension $n_u$) is the control action and $y$ (of dimension $n_y$) is the measured output. The sizes of matrices in (3) are assumed to be compatible with associated signal sizes.
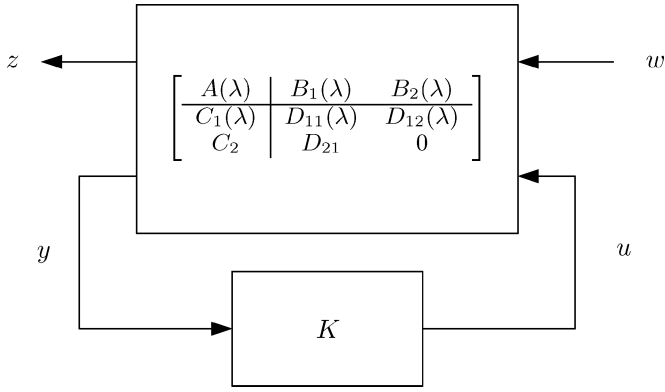
Fig. 6. A generalized plant with an uncertain parameter vector $\lambda$ and a controller $K$.

Assumptions on the plant parameters are as follows.

A.1 $(A(\lambda), B_2(\lambda), C_2)$ is stabilizable and detectable for each $\lambda \in \Lambda$.

A.2 The set $\Lambda$ is the unit simplex set:

$$\Lambda := \left\{ \lambda \in \mathbb{R}^N : \sum_{i=1}^{N} \lambda_i = 1, \lambda_i \geq 0, \quad i = 1, \dots, N \right\}.$$

A.3 The matrix-valued function $(A, B_1, B_2, C_1, D_{11}, D_{12})(\lambda)$ is linear with respect to $\lambda$.

The assumption A.1 is necessary and sufficient for each system in $\Sigma^{\Lambda}$ to be stabilizable with dynamic output feedback. The assumption A.2 is without loss of generality if the uncertain parameter set of $(A, B_1, B_2, C_1, D_{11}, D_{12})$ forms a polytope. In fact, such a polytopic uncertain set can always be reparameterized in the form of (3) using a unit simplex $\Lambda$. The assumptions A.2 and A.3 guarantee that the set of uncertain system matrices can be represented as a polytope with its vertices

$$\begin{aligned} \left( A^i, B_1^i, B_2^i, C_1^i, D_{11}^i, D_{12}^i \right) : \\ = (A, B_1, B_2, C_1, D_{11}, D_{12})(e_i), \quad \forall i \in \{1, \dots, N\} \end{aligned}$$

where $e_i$ is the $i$th unit vector. The assumption A.3 is mathematically expressed as

$$\begin{aligned} (A, B_1, B_2, C_1, D_{11}, D_{12})(\lambda) \\ = \sum_{i=1}^{N} \lambda_i \left( A^i, B_1^i, B_2^i, C_1^i, D_{11}^i, D_{12}^i \right) \end{aligned} \quad (4)$$

and necessary for the design of robust controller based on LMI techniques.

### B. Worst-Case $\mathcal{H}_2$ Performance Minimization Problem

For the set $\Sigma^{\Lambda}$ of parametric uncertain LTI systems in (3), we aim at designing a robust controller $K$:

$$K(z) := \left[ \begin{array}{c|c} A_K & B_K \\ \hline C_K & D_K \end{array} \right], \quad A_K \in \mathbb{R}^{n \times n} \quad (5)$$

such that the *worst-case $\mathcal{H}_2$ performance cost*

$$J_2(\Lambda, K) := \sup_{\lambda \in \Lambda} \|T_{zw}(\lambda, K)\|_2 \quad (6)$$

is to be minimized, where $T_{zw}(\lambda, K)$ denotes the closed-loop transfer function from the disturbance signal $w$ to the output signal $z$. Mathematically, the *worst-case $\mathcal{H}_2$ performance minimization problem* is to solve the optimization problem

$$\min_{K \in \mathcal{K}} J_2(\Lambda, K) \quad (7)$$

where $\mathcal{K}$ is the set of all controllers that internally stabilize the closed-loop system for all $\lambda \in \Lambda$.

### C. Robust $\mathcal{H}_2$ Controller Synthesis Based on LMI Techniques

Let us parameterize the controller $K$ in (5) by defining a matrix $\Theta$ as

$$\Theta := \begin{bmatrix} A_K & B_K \\ C_K & D_K \end{bmatrix} \in \mathbb{R}^{(n+n_u) \times (n+n_y)} \quad (8)$$

where the order of the controller is the same as that of the (reduced-order) plant. Then, as in [28], the closed-loop system matrix with $\lambda \in \Lambda$ can be written as an affine function of $\Theta$

$$\begin{aligned} \begin{bmatrix} A_{\mathrm{cl}}(\lambda, \Theta) & B_{\mathrm{cl}}(\lambda, \Theta) \\ C_{\mathrm{cl}}(\lambda, \Theta) & D_{\mathrm{cl}}(\lambda, \Theta) \end{bmatrix} : \\ = \begin{bmatrix} A_0(\lambda) & B_0(\lambda) \\ C_0(\lambda) & D_{11}(\lambda) \end{bmatrix} + \begin{bmatrix} B(\lambda) \\ D_{12}(\lambda) \end{bmatrix} \Theta \begin{bmatrix} C & D_{21} \end{bmatrix} \quad (9) \end{aligned}$$

where

$$A_0(\lambda) := \begin{bmatrix} A(\lambda) & 0_{n \times n} \\ 0_{n \times n} & 0_{n \times n} \end{bmatrix}; \quad B_0(\lambda) := \begin{bmatrix} B_1(\lambda) \\ 0_{n \times n_w} \end{bmatrix};$$

$$C_0(\lambda) := [C_1(\lambda) \quad 0_{n_z \times n}]; \quad B(\lambda) := \begin{bmatrix} 0_{n \times n} & B_2(\lambda) \\ I_{n \times n} & 0_{n \times n_u} \end{bmatrix};$$

$$C := \begin{bmatrix} 0_{n \times n} & I_{n \times n} \\ C_2 & 0_{n_y \times n} \end{bmatrix}; \quad D_{12}(\lambda) := [0_{n_z \times n} \quad D_{12}(\lambda)];$$

$$D_{21} := \begin{bmatrix} 0_{n \times n_w} \\ D_{21} \end{bmatrix}.$$

Using the controller parameter matrix $\Theta$, the worst-case $\mathcal{H}_2$ performance minimization problem is rewritten as[1]

$$\min_{\Theta} \max_{\lambda \in \Lambda} \|T_{zw}(\lambda, \Theta)\|_2. \quad (10)$$

This optimization problem is nonconvex, and therefore, it is difficult to solve exactly in the globally optimal sense. Next, we will explain a procedure to get a reasonable solution in a systematic way. This procedure involves two iterative decent algorithms, called $P$-$K$ iteration and $\mathcal{G}$-$K$ iteration, and is illustrated by a flowchart in Fig. 7. By a number of numerical simulations, we have found that it is generally most effective for $\mathcal{G}$-$K$ iteration to start with the final robust controller synthesized by $P$-$K$ iteration as its initial condition.

*1) P-K Iteration:* The problem in (10) can be solved by optimization subject to the standard LMI conditions for $\mathcal{H}_2$ norm. In this paper, we refer to the dual iteration algorithm used in [12], [24], [25] based on the standard LMI conditions as the $P$-$K$ iteration algorithm. A reasonable initial controller is synthesized by a method proposed in [21].

---

[1] With abuse of notation, $T_{zw}(\lambda, \Theta) := T_{zw}(\lambda, K)$
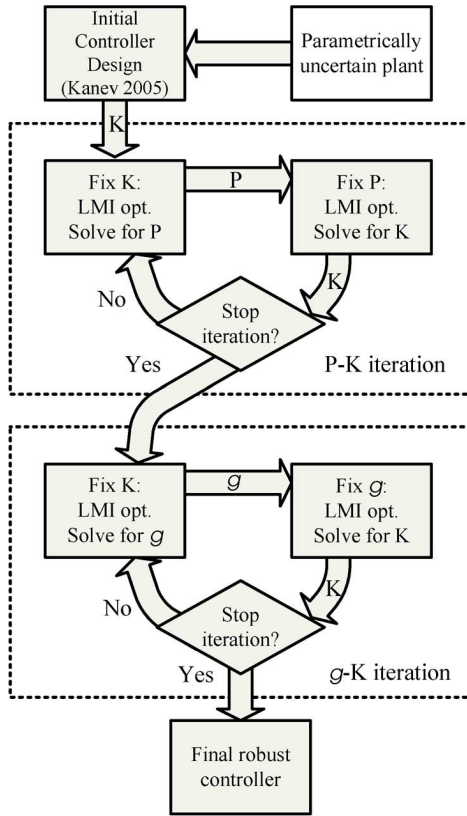
Fig. 7. The flowchart of designing a robust controller via $\mathcal{G}$-$K$ iteration.

TABLE III
COMPARISON OF NOMINAL AND WORST-CASE STABILITY MARGINS WHEN THE LOOP IS BROKEN AT $\hat{y}_{\text{PES}}, \hat{y}_m$, AND $\hat{y}_p$ FOR $P$-$K$ AND $\mathcal{G}$-$K$ ITERATION FOR THE REDUCED ORDER SYSTEM $\Sigma^\lambda$

| Broken Loop | Design Approach | Gain Margin (dB) | | Phase Margin (°) | |
|---|---|---|---|---|---|
| | | Nominal | W.C. | Nominal | W.C. |
| $\hat{y}_{PES}$ | $P$-$K$ Iteration | 3.60 | 3.59 | 34.61 | 34.50 |
| | $\mathcal{G}$-$K$ Iteration | 5.17 | 5.15 | 34.95 | 34.84 |
| $\hat{y}_m$ | $P$-$K$ Iteration | -5.58 | -5.16 | -26.73 | -25.86 |
| | $\mathcal{G}$-$K$ Iteration | 7.81 | 7.79 | -48.87 | -45.18 |
| $\hat{y}_p$ | $P$-$K$ Iteration | 10.95 | 10.18 | -88.28 | -63.49 |
| | $\mathcal{G}$-$K$ Iteration | 11.27 | 11.10 | $\infty$ | -86.34 |

*2) $\mathcal{G}$-$K$ Iteration:* The problem in (10) is solved by optimization subject to the extended LMI conditions for $\mathcal{H}_2$ norm introduced by de Oliveira [26].

$$\min_{\{W_i:i=1,\dots,N\},\{P_i:i=1,\dots,N\},\Theta,\mathcal{G},\gamma^2} \gamma^2,$$
$$\text{subject to} \quad \mathcal{M}(W_i, P_i, \Theta, \mathcal{G}, \gamma^2, e_i) \succ 0, \quad i = 1, \dots, N$$
$$(11)$$

where $\mathcal{M}(W, P, \Theta, \mathcal{G}, \gamma^2, \lambda)$ is given by

$$\mathcal{M}(W, P, \Theta, \mathcal{G}, \gamma^2, \lambda):$$
$$= (\gamma^2 - \text{trace}(W)) \oplus \begin{bmatrix} W & C_{\text{cl}}(\lambda,\Theta)\mathcal{G} & D_{\text{cl}}(\lambda,\Theta) \\ \star & \mathcal{G}+\mathcal{G}^T - P & 0 \\ \star & \star & I \end{bmatrix}$$
$$\oplus \begin{bmatrix} P & A_{\text{cl}}(\lambda,\Theta)\mathcal{G} & B_{\text{cl}}(\lambda,\Theta) \\ \star & \mathcal{G}+\mathcal{G}^T - P & 0 \\ \star & \star & I \end{bmatrix}.$$

Here, $\star$ represents entries which follow from symmetry. trace($W$) denotes the trace of $W$. $P$ and $W$ are matrices of appropriate sizes satisfying $P = P^T$ and $W = W^T$. $\mathcal{G}$ is a matrix of the same size as $P$. The closed-loop system matrices $A_{\text{cl}}, B_{\text{cl}}, C_{\text{cl}}$ and $D_{\text{cl}}$ are defined in (9).

We will explain why the conditions in (11) guarantees the worst-case $\mathcal{H}_2$ constraint $\|T_{zw}(\lambda,\Theta)\|_2 < \gamma$ for all $\lambda \in \Lambda$. Suppose that the matrix inequalities in (11) hold. Then, for any $\lambda \in \Lambda$, we have

$$\sum_{i=1}^N \lambda_i \mathcal{M}(W_i, P_i, \Theta, \mathcal{G}, \gamma^2, e_i) \succ 0.$$

Since the matrix-valued function $\mathcal{M}(W, P, \Theta, \mathcal{G}, \gamma^2, \lambda)$ is affine with respect to $W, P$, and $\lambda$, and since $\sum_{i=1}^N \lambda_i = 1$, this can be written as

$$\mathcal{M}\left(\sum_{i=1}^N \lambda_i W_i, \sum_{i=1}^N \lambda_i P_i, \Theta, \mathcal{G}, \gamma^2, \sum_{i=1}^N \lambda_i e_i\right) \succ 0, \quad \forall \lambda \in \Lambda.$$

By introducing matrices

$$W_\lambda := \sum_{i=1}^N \lambda_i W_i, \quad P_\lambda := \sum_{i=1}^N \lambda_i P_i \qquad (12)$$

and noticing

$$\text{trace}(W_\lambda) = \sum_{i=1}^N \lambda_i \text{trace}(W_i)$$

we reach a condition

$$\mathcal{M}(W_\lambda, P_\lambda, \Theta, \mathcal{G}, \gamma^2, \lambda) \succ 0, \quad \forall \lambda \in \Lambda. \qquad (13)$$

By Theorem 1 in [26], (13) implies the worst-case $\mathcal{H}_2$ constraint $\|T_{zw}(\lambda,\Theta)\|_2 < \gamma$ for all $\lambda \in \Lambda$.

The optimization problem (11) is nonconvex, due to the coupling between $\mathcal{G}$ and $\Theta$. We thus use the following coordinate descent algorithm for finding a sub-optimal robust controller:

1) [**Initial design of** $\Theta$]: Obtain the initial controller based on $P$-$K$ iteration. Set $\Theta^1$ to the result of the initial design. Also set $j = 1$.
2) [**Design of** $\mathcal{G}$]: Fix $\Theta := \Theta^j$. Solve the convex optimization problem in (11) with respect to $\gamma^2, \{W_i : i = 1, \dots, N\}, \{P_i : i = 1, \dots, N\}$ and $\mathcal{G}$. Set $\mathcal{G}^j$ to a solution $\mathcal{G}$.
3) [**Design of** $\Theta$]: Fix $\mathcal{G} := \mathcal{G}^j$. Solve the convex optimization problem in (11) with respect to $\gamma^2, \{W_i : i = 1, \dots, N\}, \{P_i : i = 1, \dots, N\}$ and $\Theta$. Set $\Theta^{j+1}$ to a solution $\Theta$. Increment $j$ by one. Continue this iteration between step 2 and step 3 until $\gamma^2$ converges.

Since the value $\gamma^2$ has a lower bound which is 0 and is monotonically non-increasing during the iterations, it will converge to some positive number.

The robust controller is optimized based on parameter dependent Lyapunov functions $V_\lambda := x_{\text{cl}}^T P_\lambda x_{\text{cl}}$, where $x_{\text{cl}}$ represents the state of the closed-loop system and $P_\lambda$ is from (13). For any $\lambda \in \Lambda, \mathcal{G}$-$K$ iteration finds a parameter dependent Lyapunov function, whereas $P$-$K$ iteration finds a common Lyapunov function for the entire uncertain set $\Lambda$. That is why $P$-$K$

TABLE IV
COMPARISON OF NOMINAL AND WORST-CASE CLOSED-LOOP RMS VALUES OF $\sqrt{z^T z}$, THE PES, $u_v$ AND $u_m$ FOR $P$-$K$ AND $\mathcal{G}$-$K$ ITERATION FOR THE REDUCED ORDER SYSTEM $\Sigma^\lambda$

| Design Approach | $\sqrt{z^T z}$ | | PES (nm) | | $u_v$ (V) | | $u_m$ (mV) | |
|---|---|---|---|---|---|---|---|---|
| | Nominal | W.C. | Nominal | W.C. | Nominal | W.C | Nominal | W.C |
| $P$-$K$ Iteration | 9.47 | 9.51 | 8.83 | 8.85 | 1.12 | 1.13 | 324 | 329 |
| $\mathcal{G}$-$K$ Iteration | 8.88 | 8.88 | 8.31 | 8.32 | 1.05 | 1.05 | 293 | 294 |

TABLE V
COMPARISON OF NOMINAL AND WORST-CASE CLOSED-LOOP RMS VALUES OF $\sqrt{z^T z}$, THE PES, $u_v$ AND $u_m$ FOR $P$-$K$ AND $\mathcal{G}$-$K$ ITERATION FOR THE FULL ORDER SYSTEM

| Design Approach | $\sqrt{z^T z}$ | | PES (nm) | | $u_v$ (mV) | | $u_m$ (mV) | |
|---|---|---|---|---|---|---|---|---|
| | Nominal | W.C. | Nominal | W.C. | Nominal | W.C | Nominal | W.C |
| $P$-$K$ Iteration | 9.52 | 10.52 | 8.88 | 9.92 | 1.14 | 1.16 | 324 | 333 |
| $\mathcal{G}$-$K$ Iteration | 8.90 | 9.37 | 8.34 | 8.82 | 1.06 | 1.10 | 294 | 299 |

iteration normally yields a more conservative controller design than $\mathcal{G}$-$K$ iteration does. Therefore, the optimization based on the extended LMI conditions in (11) will improve the worst-case performance as compared to the one based on the standard LMI conditions in [12], [24], [25].

## IV. ROBUST $\mathcal{H}_2$ CONTROLLERS IN THE HDD EXAMPLE

In this section, controllers were designed for a reduced-order HDD servo system, and they were evaluated for the full-order system. Using $P$-$K$ iteration, the controller $K_{PK}$ was designed for $\Sigma^\Lambda$. This controller was then refined using $\mathcal{G}$-$K$ iteration to produce the controller $K_{\mathcal{G}K}$ as suggested by the flowchart in Fig. 7.

### A. Performance Evaluation

To analyze each controller, the control loop was closed for each of 400 samples of $\Sigma^\Lambda$ which were generated by randomly selecting values of $\lambda \in \Lambda$. For each closed-loop system, stability was verified and stability margins were computed when the loop was broken at each of three locations: $\hat{y}_{\text{PES}}, \hat{y}_m$, and $\hat{y}_p$. Table III shows the nominal and worst-case (in absolute value) stability margins for both controllers. Since negative gain margins correspond to phase crossover frequencies at which the loop gain is larger than 1, negative gain margins mean that stability of the loop is most sensitive to loop gain reduction. Negative phase margins can be interpreted similarly. Although both controllers achieve reasonable stability margins, $K_{\mathcal{G}K}$ achieves considerably larger nominal and worst-case stability margins. To evaluate the robust performance of the closed-loop system, the RMS values of the PES, $u_v$, and $u_m$ were computed for each closed-loop system sample. Table IV shows the nominal and worst-case closed-loop RMS values of these three signals for both controllers. For $K_{PK}$ and $K_{\mathcal{G}K}$, the degradation from the nominal RMS values of the relevant signals to their worst-case values is less than 1.6% and 0.4%, respectively. This verifies that although the performance for both controllers is robust in the time domain, $K_{\mathcal{G}K}$ achieves performance which degrades much less over $\lambda \in \Lambda$. Also, relative to $K_{PK}$, $K_{\mathcal{G}K}$ achieves 6%, 7%, and 10% improvements in the worst case RMS values of the PES, $u_v$, and $u_m$, respectively.
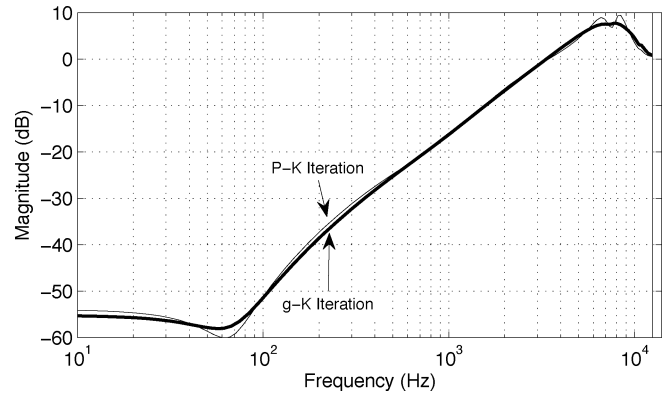


Fig. 8. Nominal closed-loop sensitivity plots for reduced order plants with controllers designed using $P$-$K$ and $\mathcal{G}$-$K$ iteration.

Fig. 8 shows the nominal closed-loop Bode plots of the sensitivity functions (from $r$ to the PES) for the systems with $K_{PK}$ and $K_{\mathcal{G}K}$. The closed-loop system with $K_{\mathcal{G}K}$ has better runout rejection properties at low frequencies and at high frequencies near the sensitivity peak. We now examine the perturbed sensitivity functions. Since the plant has little uncertainties at low frequencies, it is only meaningful to examine the perturbed sensitivity plots at high frequencies. Fig. 9 shows the closed-loop sensitivity plots of the systems with $K_{PK}$ and $K_{\mathcal{G}K}$ for 50 random samples of $\lambda \in \Lambda$. Note that although $\lambda$ has little effect on the closed-loop sensitivity function in both closed-loop systems, the closed-loop system with $K_{\mathcal{G}K}$ has less variation in its sensitivity function over $\lambda \in \Lambda$. Also note that the worst-case closed-loop sensitivity crossover frequency is higher than 3.3 kHz in both cases.

To further validate our design, we checked the performance of the full 19th order model with the designed controllers. To do this, we first chose 400 random samples of $\bar{\bar{\Sigma}}_C^{\bar{\Lambda}^c}$, discretized each sample, and then closed the control loop for each of these samples. The stability of each closed-loop system sample was verified and the RMS values of the PES, $u_v$, and $u_m$ were computed. Table V shows the nominal and worst-case closed-loop RMS values of these three signals for both controllers. For $K_{PK}$ and $K_{\mathcal{G}K}$, the degradation from the nominal RMS values of the relevant signals to their worst case values is less than 12% and
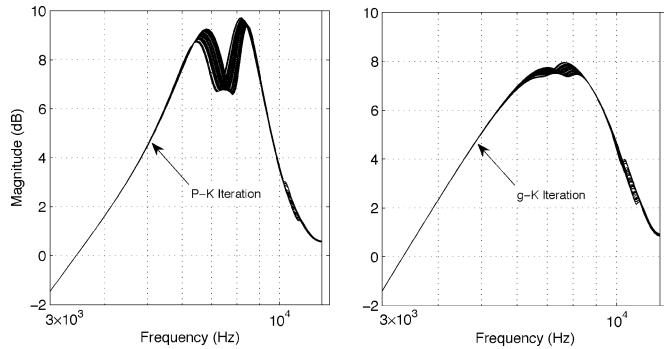
Fig. 9. Closed-loop sensitivity plots for reduced order plants with controllers designed using $P$-$K$ and $\mathcal{G}$-$K$ iteration for 50 random samples of $\lambda \in \Lambda$.

6%, respectively. This verifies that although the performance for both controllers is robust in the time domain, $K_{\mathcal{G}K}$ achieves performance which degrades much less over the uncertain parameter set. Also, relative to $K_{PK}$, $K_{\mathcal{G}K}$ achieves 11%, 5%, and 10% improvements in the worst case RMS values of the PES, $u_v$, and $u_m$, respectively.

## V. CONCLUSION

This paper presented the $\mathcal{G}$-$K$ iteration technique for robust track-following control in HDDs. This approach utilized robust controller design techniques for polytopic parametric uncertain LTI systems based on parameter dependent Lyapunov functions. The robust output-feedback controller was optimized for the $\mathcal{H}_2$ worst-case performance of a discrete-time system under convex polytopic parametric uncertainties, based on the extended LMI condition introduced by de Oliveira [26]. The $\mathcal{G}$-$K$ iteration algorithm was applied for optimization of the robust controller to guarantee monotonic non-increase of the worst-case performance during iterations. We have applied the synthesis algorithm to design a robust $\mathcal{H}_2$ track-following controller for a dual-stage servo system in HDDs, which showed the improvement of robust track-following performance as compared to ones used in [12], [24], and [25].

## REFERENCES

[1] A. Al Mamun, G. Guo, and C. Bi, *Hard Disk Drive: Mechatronics and Control*. Boca Raton, FL: CRC, 2007.

[2] K. Peng, B. M. Chen, T. H. Lee, and V. Venkataramanan, *Hard Disk Drive Servo Systems*, 2nd ed. Berlin, Germany: Springer, 2006.

[3] I. Mareels, T. Suthasun, and A. Al-Mamun, "System identification and controller design for dual actuated hard disk drive," *Control Eng. Practice*, vol. 12, no. 6, pp. 665–676, June 2004.

[4] G. Peng, M. Wang, H. Zhang, and X. Huang, "Dual-stage HDD head positioning using an $\mathcal{H}_\infty$ almost disturbance decoupling controller and a tracking differentiator," *J. Mechatronics*, vol. 19, no. 5, pp. 788–796, Aug. 2009.

[5] J. Schroceck and W. C. Messner, "On compensator design for linear time-invariant dual-input single-output systems," *IEEE/ASME Trans. Mechatronics*, vol. 6, no. 1, pp. 50–57, 2001.

[6] J. Hong, T. Semba, T. Hirano, and L.-S. Fan, "Dual-stage servo controller for HDD using mems microactuator," *IEEE Trans. Magn.*, vol. 35, no. 5, pp. 2271–2273, Sep. 1999.

[7] K. W. Chan and W. Liao, "Shock resistance of a disk-drive assembly using piezoelectric actuators with passive damping," *IEEE Trans. Magn.*, vol. 44, no. 4, pp. 525–532, Apr. 2008.

[8] H. T. Loh, Z. He, and E. H. Ong, "Reliability evaluation of piezoelectric micro-actuators with application in hard disk drives," *IEEE Trans. Magn.*, vol. 44, no. 11, pp. 3722–3725, Nov. 2008.

[9] K. Oldham, X. Huang, A. Chahwan, and R. Horowitz, "Design, fabrication, and control of a high-aspect ratio microactuator for vibration suppression in a hard disk drive," in *Proc. 16th IFAC World Congress*, Prague, 2005.

[10] S. Kon, K. Oldham, R. Ruzicka, and R. Horowitz, "Design and fabrication of a piezoelectric instrumented suspension for hard disk drives," in *Proc. SPIE, Smart Structures and Materials 2006: Sensors and Smart Structures Technologies for Civil, Mechanical, and Aerospace Systems*, 2006, pp. 951–960.

[11] B. Liu, S. H. Leong, K. W. Ng, Z. Yuan, and T. Chong, "Method for in situ motion measurement of head-slider in both flying height and off-track directions," *IEEE Trans. Magn.*, vol. 44, no. 5, pp. 640–642, May 2008.

[12] R. A. De Callafon, R. Nagamune, and R. Horowitz, "Robust dynamic modeling and control of dual-stage actuators," *IEEE Trans. Magn.*, vol. 42, no. 2, pp. 247–254, Feb. 2006.

[13] X. Huang and R. Horowitz, "Robust control of dual-stage servo systems in hard disk drives: Methodology development, comparative study, and experimental verification," *VDM Verlag*, May 2008.

[14] S. Felix, R. Conway, and R. Horowitz, "Model reduction and parametric uncertainty identification for robust h2 control synthesis for dual-stage hard disk drives," *IEEE Trans. Magn.*, vol. 43, no. 9, pp. 3763–3768, Sep. 2007.

[15] R. A. De Callafon, M. R. Graham, and L. Shrinkle, "Modeling and low-order control of hard disk drives with considerations for product variability," *IEEE Trans. Magn.*, vol. 42, no. 10, pp. 2588–2590, Oct. 2006.

[16] J. Choi, R. Nagamune, and R. Horowitz, "Multiple robust track-following controller design in hard disk drives," *Int. J. Adaptive Control Signal Process.*, vol. 22, no. 4, 2008.

[17] Q. W. Jia, "Disturbance rejection through disturbance observer with adaptive frequency estimation," *IEEE Trans. Magn.*, vol. 45, no. 6, pp. 2675–2678, Jun. 2009.

[18] P. A. Ioannou, J. Levin, N. O. Prez-Arancibia, and T. Tsao, "A neural-networks-based adaptive disturbance rejection method and its application to the control of hard disk drives," *IEEE Trans. Magn.*, vol. 45, no. 5, pp. 2140–2150, May 2009.

[19] G. Guo, C. K. Pang, W. E. Wong, and B. M. Chen, "Nonrepeatable run-out rejection using online iterative control for high-density data storage," *IEEE Trans. Magn.*, vol. 43, no. 5, pp. 2029–2037, May 2007.

[20] X. Huang, R. Nagamune, and R. Horowitz, "A comparison of multirate robust track-following control synthesis techniques for dual-stage and multi-sensing servo systems in hard disk drives," *IEEE Trans. Magn.*, vol. 42, no. 7, pp. 1896–1904, Jul. 2006.

[21] S. Kanev, C. Scherer, M. Verhaegen, and B. De Shutter, "Robust output-feedback controller design via local BMI optimization," *Automatica*, vol. 40, pp. 1115–1127, 2004.

[22] M. Fukuda and M. Kojima, "Branch-and-cut algorithms for the bilinear matrix inequality eigenvalue problem," *Comput. Optim. Appl.*, vol. 19, pp. 79–105, 2001.

[23] T. Iwasaki, "The dual iteration for fixed order control," *IEEE Trans. Automatic Control*, vol. 44, no. 4, pp. 783–788, 1999.

[24] R. Nagamune, X. Huang, and R. Horowitz, "Robust control synthesis techniques for multirate and multi-sensing track-following servo systems in hard disk drives," *ASME J. Dyn. Syst. Meas. Control*, vol. 132, Mar. 2005.

[25] R. Nagamune, X. Huang, and R. Horowitz, "Multirate track-following control with robust stability for a dual-stage multi-sensing servo system in HDDs," in *44th IEEE Conf. Decision and Control, 2005 and 2005 Eur. Control Conf. CDC-ECC'05*, 2005, pp. 3886–3891.

[26] M. C. De Oliveira, J. C. Geromel, and J. Bernussou, "Extended $\mathcal{H}_2$ and $\mathcal{H}_\infty$ norm characterizations and controller parametrizations for discretetime systems," *Int. J. Control*, vol. 75, no. 9, pp. 666–679, June 2002.

[27] R. A. De Callafon, R. Nagamune, and R. Horowitz, "Robust dynamic modeling and control of dual-stage actuators," *IEEE Trans. Magn.*, vol. 42, no. 2, pp. 247–254, Feb. 2006.

[28] P. Gahinet and P. Apkarian, "A linear matrix inequality approach to $\mathcal{H}_\infty$ control," *Int. J. Robust Nonlinear Control*, vol. 40, pp. 421–448, 1994.

**Richard Conway** (S'09) received the B.S. and M.S. degrees in mechanical engineering from the University of California at Berkeley in 2004 and 2008, respectively. Currently, he is pursuing the Ph.D. degree in mechanical engineering under the guidance of Prof. Roberto Horowitz. His research interests include optimal robust performance control, algorithms for system analysis and controller synthesis, Riccati equations in control, convex optimization in control, periodic discrete-time systems, identification of parametrically uncertain systems, and model reduction.

Mr. Conway is a student member of ASME.

**Jongeun Choi** (S'05–M'06) received the Ph.D. and M.S. degrees in mechanical engineering from the University of California at Berkeley in 2006 and 2002, respectively, and the B.S. degree in mechanical design and production engineering from Yonsei University, Seoul, Republic of Korea, in 1998.

He is currently an Assistant Professor with the Departments of Mechanical Engineering, and Electrical and Computer Engineering at Michigan State University, East Lansing. His research interests include adaptive, distributed and robust control and statistical learning algorithms, with applications to self-organizing systems, mobile robotic sensors, environmental adaptive sampling, and biomedical problems.

Dr. Choi is a member of ASME. He received an NSF CAREER Award in 2009.

**Ryozo Nagamune** (S'97–M'03) received the B.S. and M.S. degrees from the Department of Control Engineering, Osaka University, Japan, in 1995 and 1997, respectively, and the Ph.D. degree from the Division of Optimization and Systems Theory, Royal Institute of Technology, Stockholm, Sweden, in 2002.

From January 2003 to June 2006, he was a postdoctoral researcher at the Mittag-Leffler Institute in Sweden, the University of California at Berkeley, and the Royal Institute of Technology in Sweden. He is currently an Assistant Professor in the Department of Mechanical Engineering, University of British Columbia, Vancouver, Canada. His research interests are robust control theory and its application to mechanical control systems, spectral estimation, and model reduction.

Dr. Nagamune is a member of ASME, and serves as a Chair of the IEEE Control Systems Society Vancouver Chapter.

**Roberto Horowitz** (M'98–SM'02) received the B.S. degree with highest honors in 1978 and the Ph.D. degree in mechanical engineering in 1983 from the University of California at Berkeley.

In 1982 he joined the Department of Mechanical Engineering at the University of California at Berkeley, where he is currently a Professor and the James Fife Endowed Chair. He teaches and conducts research in the areas of adaptive, learning, nonlinear and optimal control, with applications to micro-electromechanical systems (MEMS), computer disk file systems, robotics, mechatronics, and Intelligent Vehicle and Highway Systems (IVHS).

Dr. Horowitz is a member of ASME.